Aeroelastic Flutter Produces Hummingbird Feather Songs
Christopher J. Clark, *et al.*
Science **333**, 1430 (2011);
DOI: 10.1126/science.1205222

indicates the presence of basal slip, because the pattern of enhanced flow is quite different from the pattern of large deformational velocity. A doubling of A does not improve the model fit (fig. S4). In a second simulation, we calculate the deformational velocity obtained for a rigid bed (*21*), that is, where the speed only depends on the power of the driving stress, but the agreement between measured and deformational velocity is not improved (fig. S5). We conclude that basal slip is a significant component of ice motion in Antarctica, which develops at the flanks of ice divides.

This organization of ice sheet flow into a complex set of meandering, size-varying, speed-varying, anastomosing tributaries most certainly dominated by basal-slip motion challenges the view of ice sheet flow constrained by internal deformation and disconnected from the coastal regions, that was adopted as the background model for continental-scale ice sheet modeling (*6*, *21*). Actual observations of continental-scale ice motion reveal a new flow regime that initiates near topographic divides and involves a substantial amount of basal-slip motion. Much remains to be understood about the mechanisms of basal motion and patterned enhanced flow, but our observations already imply a tighter connection between coastal sectors and interior regions than in the hypothetical case of a uniform ice sheet flow, because the concentration of ice fluxes along preferred channels enhances the diffusivity of perturbations. It is likely that this patterned enhanced flow is not unique to Antarctica but is a common feature of ice sheets. The mapping of Antarctic ice motion therefore redefines our view of ice sheet flow dynamics and the way ice sheets have been modeled in the past, with implications for improving reconstructions of past and ongoing changes and especially for modeling the evolution of ice sheet dynamics in a warming climate.

References and Notes

1. R. M. Goldstein, H. Engelhardt, B. Kamb, R. M. Frolich, *Science* **262**, 1525 (1993).
2. E. Rignot *et al.*, *Nat. Geosci.* **1**, 106 (2008).
3. J. L. Bamber, D. G. Vaughan, I. Joughin, *Science* **287**, 1248 (2000).
4. A. M. Le Brocq, A. J. Payne, M. J. Siegert, *Comput. Geosci.* **32**, 1780 (2006).
5. J. L. Bamber, E. Rignot, *J. Glaciol.* **48**, 237 (2002).
6. P. Lemke *et al.*, in *Climate Change 2007: The Physical Science Basis. Contribution of Working Group I to the Fourth Assessment Report of the Intergovernmental Panel on Climate Change*, S. Solomon *et al.*, Eds. (Cambridge Univ. Press, Cambridge, 2007).
7. K. C. Jezek, K. Farness, R. Carande, X. Wu, N. Labelle-Hammer, *Radio Sci.* **38**, 8067 (2003).
8. J. L. Bamber, J. Gomez-Dans, *Earth Planet. Sci. Lett.* **237**, 516 (2005).
9. E. Rignot *et al.*, *Geophys. Res. Lett.* **31**, L18401 (2004).
10. C. W. Swithinbank, in *Satellite Image Atlas of Glaciers of the World*, U.S. Geological Survey Professional Paper no. 1386-B (1988).
11. F. Pattyn, S. De Brabander, A. Huyghe, *Ann. Glaciol.* **40**, 225 (2005).
12. I. Allison, R. Frew, I. Knight, *Polar Rec.* **21**, 241 (1982).
13. A. Jenkins, S. S. Jacobs, *J. Geophys. Res.* **113**, C04013 (2008).
14. I. Joughin *et al.*, *Science* **286**, 283 (1999).
15. M. Stenoien, C. R. Bentley, *J. Geophys. Res.* **105**, 21761 (2000).
16. D. M. Rippin, J. L. Bamber, M. J. Siegert, D. G. Vaughan, H. F. J. Corr, *J. Geophys. Res.* **108**, 6008 (2003).
17. J. L. Bamber *et al.*, *Geology* **34**, 33 (2006).
18. R. E. Bell, M. Studinger, C. A. Shuman, M. A. Fahnestock, I. Joughin, *Nature* **445**, 904 (2007).
19. R. Kwok, M. J. Siegert, F. D. Carsey, *J. Glaciol.* **46**, 689 (2000).
20. N. F. Mc Intyre, *J. Glaciol.* **31**, 99 (1985).
21. K. Cuffey, W. S. B. Paterson, *The Physics of Glaciers* (Academic Press, Amsterdam, ed. 4, 2010).
22. T. Haran, J. Bohlander, T. Scambos, T. Painter, M. Fahnestock, MODIS (Moderate-Resolution Imaging Spectradiometer) mosaic of Antarctica (MOA) image map (digital media) (National Snow and Ice Data Center, Boulder, CO, 2006).
23. E. Rignot, J. Mouginot, B. Scheuchl, *Geophys. Res. Lett.* **38**, L10504 (2011).
24. M. B. Lythe, D. G. Vaughan, *J. Geophys. Res.* **106**, 11335 (2001).

Acknowledgments: This work was performed at the University of California Irvine and at Caltech's Jet Propulsion Laboratory under a contract with the National Aeronautics and Space Administration's MEaSUREs and Cryospheric Science Programs. Data acquisitions are courtesy of the IPY Space Task Group. The digital ice motion map will be available as a MEaSUREs Earth Science Data Record (ESDR) at the National Snow and Ice Data Center, Boulder, CO. We thank two anonymous reviewers for their comments.

Supporting Online Material

www.sciencemag.org/cgi/content/full/science.1208336/DC1
Materials and Methods
Figs. S1 to S5
Table S1
References (*25*–*31*)

13 May 2011; accepted 27 July 2011
Published online 18 August 2011;
10.1126/science.1208336

Aeroelastic Flutter Produces Hummingbird Feather Songs

Christopher J. Clark,[1] Damian O. Elias,[2] Richard O. Prum[1]

During courtship flights, males of some hummingbird species produce diverse sounds with tail feathers of varying shapes. We show that these sounds are produced by air flowing past a feather, causing it to aeroelastically flutter and generate flutter-induced sound. Scanning laser doppler vibrometery and high-speed video of individual feathers of different sizes and shapes in a wind tunnel revealed multiple vibratory modes that produce a range of acoustic frequencies and harmonic structures. Neighboring feathers can be aerodynamically coupled and flutter either at the same frequency, resulting in sympathetic vibrations that increase loudness, or at different frequencies, resulting in audible interaction frequencies. Aeroelastic flutter is intrinsic to stiff airfoils such as feathers and thus explains tonal sounds that are common in bird flight.

Feathers were a key innovation in the evolution of bird flight, providing a stiff, lightweight aerodynamic surface, or airfoil (*1*). As early designers of aircraft discovered, stiff, light airfoils in fast-flowing air are prone to aeroelastic flutter, whereby the airfoil oscillates at a frequency set by its stiffness and inertia, and aerodynamic forces (*2*). The acoustics of flutter is incompletely understood (*3*). However, in many birds, modified flight feathers are associated with the production of tonal flight sounds used in communication such as courtship displays (as in hummingbirds or snipe).

Hummingbirds are a clade of ~330 polygynous species in which males court females with showy ornaments, aerobatic displays, and vocal songs; females choose a mate from among available males (*4*). Independent of the humming of the wings for which hummingbirds are famous, males of the ~35 species in the "bee" hummingbird clade (*5*) produce tonal flight sounds, or courtship songs, during dive displays for females visiting their courtship territories. Although dive kinematics vary, a male generally ascends 5 to 40 m and then swoops down at high speed past the perched female, rapidly spreading and shutting his tail at the nadir of the dive and producing dive sounds in synchrony with each tail spread (*6*–*9*). In previous work, we have shown that tail feathers (or rectrices; R1, innermost, through R5, outermost) are both necessary and sufficient for the production of dive sounds: Experimental manipulation of specific tail feathers silences a male's dive sound, whereas these same feathers are sufficient to recreate the dive sound in lab experiments (*6*–*9*). We proposed that these dive sounds are produced by flutter (*6*) but did not measure flutter directly. In this work, we measured the vibrations of an array of hummingbird tail feathers in a wind tunnel directly, using a scanning laser doppler vibrometer (SLDV). We describe how aeroelastic flutter can result in a diverse array of audible sounds.

Air flowing past a feather provides aerodynamic energy that can cause flutter. We tested the relationship between air velocity (U_{air}) and feather

[1]Department of Ecology and Evolutionary Biology and Peabody Museum of Natural History, Post Office Box 208105, Yale University, New Haven, CT 06520, USA. [2]Environmental Science and Policy and Management, 137 Mulford Hall, University of California, Berkeley, Berkeley, CA 94720, USA.

vibration velocity ($V_{feather}$) by mounting individual rectrices in a wind tunnel across a range of U_{air} values (*10*). Far-field sound was recorded with a microphone while SLDV sequentially measured $V_{feather}$ of ~100 points across the feather. We tested 31 feathers from males of 14 species, including 24 feathers known or suspected to produce display sounds and 7 others that may not produce sounds in wild birds [see supporting online methods (*10*), fig. S1, and table S1].

SLDV allowed characterization of the onset and development of feather flutter with increasing U_{air}. $V_{feather}$ exhibited distinct differences in behavior over three ranges of U_{air} (Fig. 1A). At low U_{air} (range I), the feather vane was immobile. At higher U_{air} (range II), minute values for $V_{feather}$ were detected in specific parts of the feather (such as the tip or trailing edge), but no measurable sounds were detected. Multiple vibratory frequencies across different regions of the feather were often simultaneously present, and small changes in U_{air} resulted in somewhat unpredictable changes in frequency and feather region(s) activated by airflow. Above a critical velocity (U^*, range III), $V_{feather}$ dramatically increased as one mode of vibration established a stable oscillation (Fig. 1A) with harmonics. Far-field sound was detected by the microphone only at air speeds above U^*, which varied from 6.7 to 19.6 m s^{-1}. All feathers exhibited stable flutter and accompanying sound above U^*, including the seven feathers that do not produce display sounds (table S1). The range of U_{air} tested included speeds greater than the birds achieve during dives (Fig. 1B), but all U^* values corresponded to behaviorally relevant flight speeds.

Above U^*, loudness increased with U_{air} (range IIIa: Fig. 1B), but at even higher U_{air}, loudness was uncorrelated or negatively correlated with U_{air} (range IIIb: Fig. 1B) (*11*). Loudness was correlated with $V_{feather}$ (Fig. 1C). Normally, both odd and even harmonics were present, but occasionally other patterns were observed such as only odd harmonics, as would be expected for a vibrating bar clamped at one end. Harmonics occasionally contained more energy than the fundamental frequency (Fig. 1D), and >30 integer harmonics were present in some cases (Fig. 1E). All feathers were compact sound sources; that is, sound wavelengths exceeded feather dimensions (*12*). Consequently, there is a nearly 1:1 relationship between

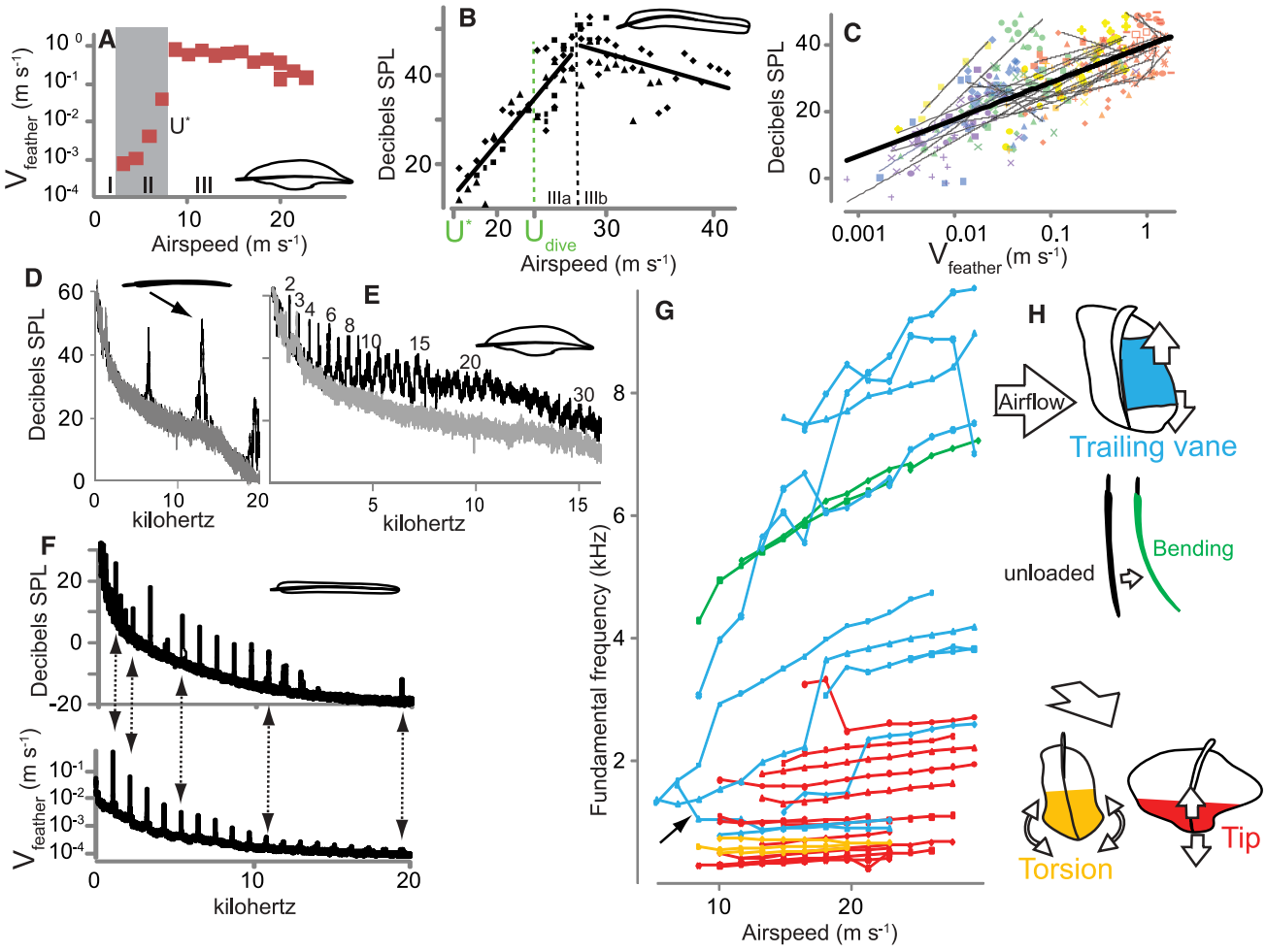

Fig. 1. Characterization of sound and vibration of single feathers in airflow. (**A**) Feather flutter velocity ($V_{feather}$) against airspeed of *S. flammula* R2. Range I: feather is immobile; range II: minute vibrations without detectable sound; range III: vibration amplitude increases sharply above a critical velocity (U^*) and sound is detected. (**B**) Sound pressure level (SPL)–airspeed relationship of *C. anna* R5 above U^* (n = 3 feathers). In range IIIa, sound pressure level rises with airspeed (slope: 2.9 dB m s^{-1}), whereas in IIIb it declines. U_{dive}, speed that live birds reach in a dive (*21*) [see (11)]. (**C**) SPL of 31 feathers from 14 species of hummingbird as a function of $V_{feather}$. Faint lines are regressions for individual feathers. Color indicates the fundamental frequency of sound (in kilohertz): red, <0.95, orange, 0.96 to 1.55, yellow, 1.56 to 2.41, green, 2.42 to 4.8, blue, 4.9 to 7.2, purple, >7.3. (**D** and **E**) Sound frequency power spectra for (D) R4 of *Chaetocercus mulsant* and (E) R2 of *S. flammula* in the wind tunnel (black) against background sound of the tunnel (gray; U_{air} = 22 m s^{-1}). (D) Second harmonic is dominant (arrow). (E) Over 30 integer harmonics are present (select harmonics are numbered). (**F**) Power spectra of *Calliphlox mitchellii* R5 in the wind tunnel (11.6 m s^{-1}); sound recording is above, and SLDV of feather flutter is below. All sounds were present as vibrations in the feather (as in arrows). (**G**) Fundamental frequency and mode of vibration of 31 different hummingbird feathers. Frequency tends to increase with airspeed, but a negative slope is possible (e.g., arrow = *C. mitchellii* R4). (**H**) Four modes of vibration: a transverse mode of the trailing vane (blue), whole-feather bending mode (green), and torsional-transverse mode of the tip (red), which in *Stellula calliope* was sometimes a purely torsional mode (yellow). See movie S1.

feather flutter and radiated sound. All far-field sound including harmonics had a corresponding vibration in the feather, although in some cases an acoustic frequency was much weaker than the corresponding flutter frequency (Fig. 1F). Frequency scaled positively with U_{air} in most but not all feathers (Fig. 1G).

Different feather shapes (Figs. 1H and 2) exhibit different modes and frequencies of vibration. We identified four types of modes of vibration (Fig. 1G and movie S1). The two most common modes of vibration were a transverse mode associated with the trailing edge of the vane, which tended to be produced by feathers with uniform width (Fig. 2), and a torsional and transverse combination associated with the feather's tip, which was exhibited in feathers with tapered or emarginated tips (Fig. 2). We also observed purely torsional modes in Calliope hummingbird (*Stellula calliope*) rectrices, and a whole-feather bending mode in the wire-shaped rectrices of the white-bellied woodstar (*Chaetocercus mulsant*) (Fig. 1G and movie S1).

The SLDV experiments were conducted with a single feather orientation intended to match the orientation of the feather in a diving bird. Small changes in orientation [and other boundary conditions (*10*)] often rendered a vibratory mode active or inactive at a given U_{air}. Most feathers had multiple modes and multiple frequencies active across different orientations and airspeeds.

If airflow can cause individual feathers to oscillate at an intrinsic resonant frequency, we predict that adjacent vibrating feathers may act as coupled oscillators, resulting in nonlinear interactions. We demonstrated two such types of coupled feather-feather interactions.

Sympathetic vibrations occur when a passive oscillator responds to external vibrations from a nearby oscillator with similar resonance characteristics. Anna's hummingbird (*Calypte anna*) generates a loud 4-kHz dive sound with R5 (Fig. 3, A and B) (*6*). Experimental removal of the adjacent R4 reduces the loudness of the dive sound but does not eliminate it (Fig. 3B) (*6*), suggesting that R4 amplifies the dive sound. R5 by itself produced a ~4-kHz sound, whereas a solitary R4 produced a ~1-kHz tone in the wind tunnel (movie S2). When R4 was placed behind (but not touching) R5, the presence of R4 increased the overall loudness by four times (12 dB; Fig. 3C and movie S2), because R4 vibrated at ~4 kHz (Fig. 3D). An alternative mechanism could be that R4 reduces "acoustic short-circuiting" of R5 (*13*). This hypothesis can be rejected because a flat aluminum plate in the shape and position of R4 did not produce a similar increase in volume (Fig. 3D).

Adjacent flight feathers may also each flutter at a different frequency. If two feathers with resonant frequencies f_1 and f_2 are aerodynamically coupled, the sum and difference ($f_2 \pm f_1$) heterodyne frequencies are expected in both

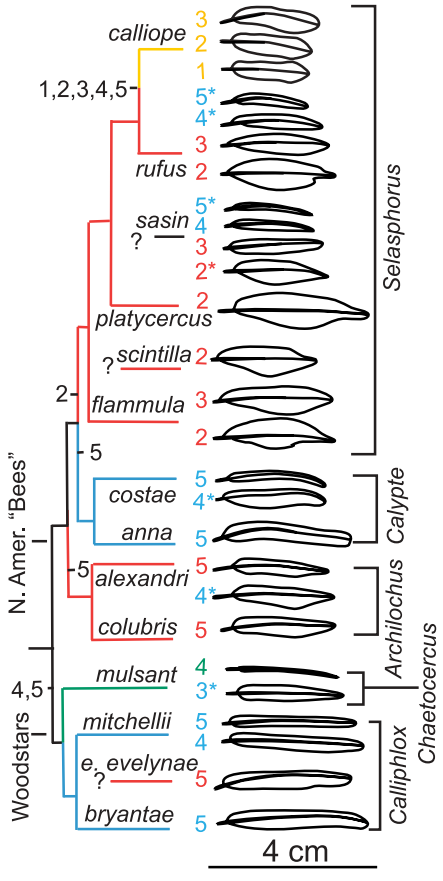

Fig. 2. Evolution of tail feather sound production in bee hummingbirds [phylogeny from (*5*)]. Outlines traced from tail feathers tested in this study are shown; colored numbers indicate rectrix identity and the mode we elicited in the wind tunnel (colors are as in Fig. 1H); the asterisk indicates feathers that may not make sound in wild birds (table S1). Lineage color indicates inferred mode of vibration (black indicates ambiguous), and the black numbers indicate which tail feather(s) produce sound.

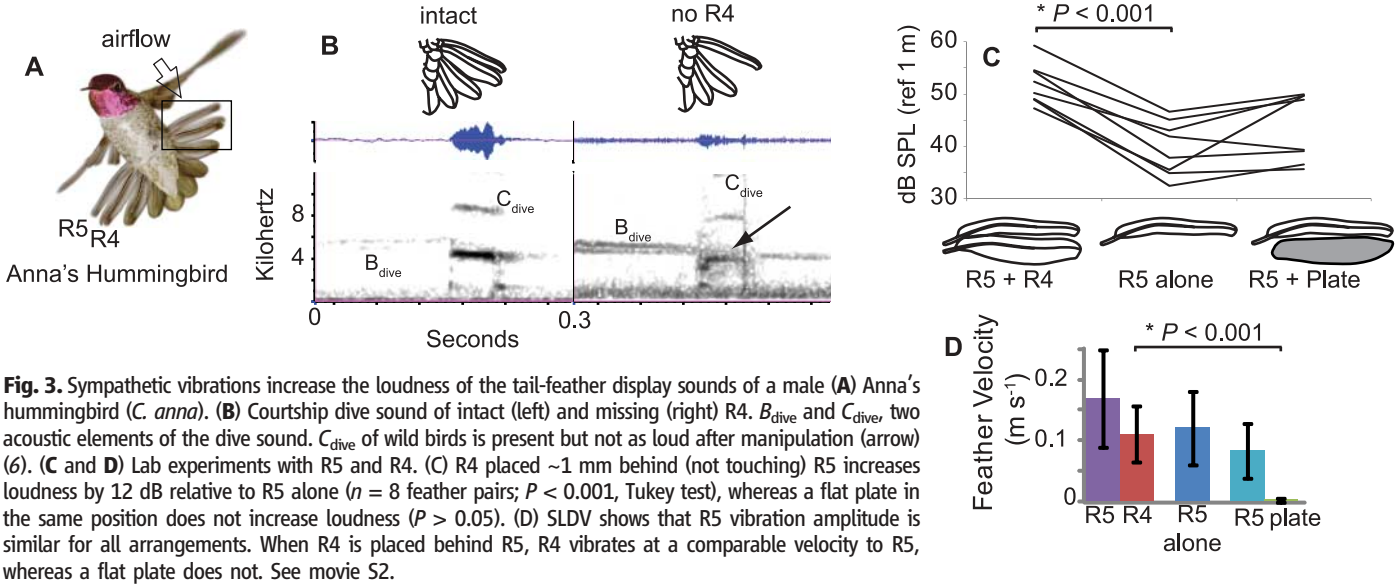

Fig. 3. Sympathetic vibrations increase the loudness of the tail-feather display sounds of a male (**A**) Anna's hummingbird (*C. anna*). (**B**) Courtship dive sound of intact (left) and missing (right) R4. B_{dive} and C_{dive}, two acoustic elements of the dive sound. C_{dive} of wild birds is present but not as loud after manipulation (arrow) (*6*). (**C** and **D**) Lab experiments with R5 and R4. (C) R4 placed ~1 mm behind (not touching) R5 increases loudness by 12 dB relative to R5 alone (n = 8 feather pairs; $P < 0.001$, Tukey test), whereas a flat plate in the same position does not increase loudness ($P > 0.05$). (D) SLDV shows that R5 vibration amplitude is similar for all arrangements. When R4 is placed behind R5, R4 vibrates at a comparable velocity to R5, whereas a flat plate does not. See movie S2.

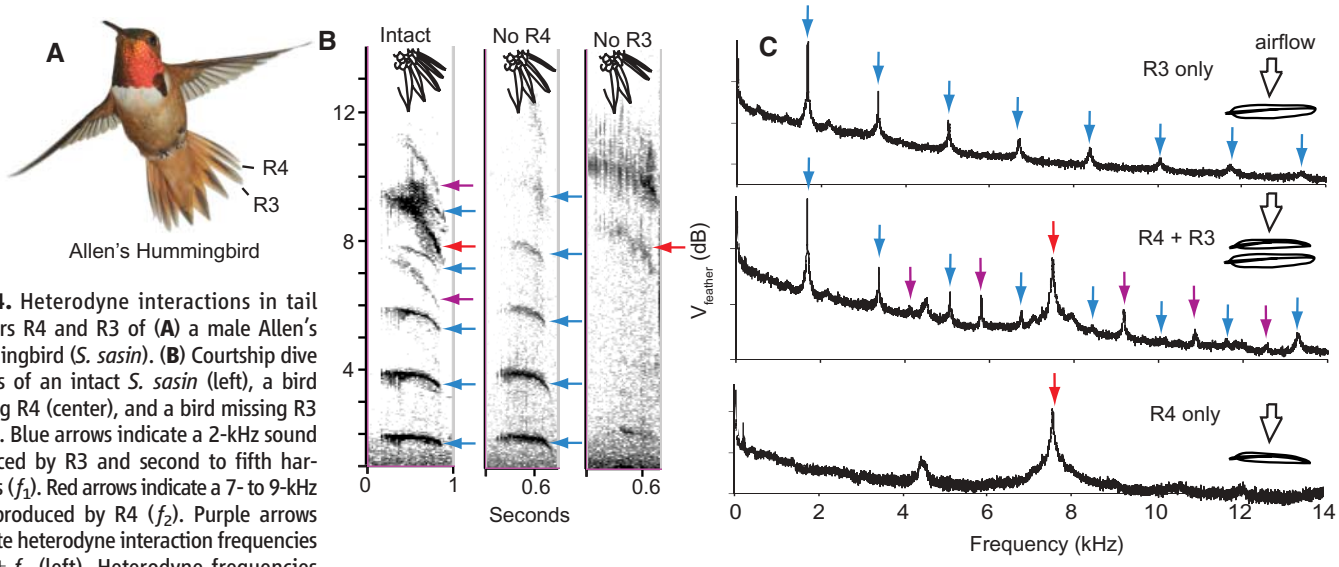

Fig. 4. Heterodyne interactions in tail feathers R4 and R3 of (**A**) a male Allen's hummingbird (*S. sasin*). (**B**) Courtship dive sounds of an intact *S. sasin* (left), a bird missing R4 (center), and a bird missing R3 (right). Blue arrows indicate a 2-kHz sound produced by R3 and second to fifth harmonics (f_1). Red arrows indicate a 7- to 9-kHz tone produced by R4 (f_2). Purple arrows indicate heterodyne interaction frequencies of $f_2 \pm f_1$ (left). Heterodyne frequencies disappear with removal of either rectrix (center and right). (**C**) Vibration frequency spectra from SLDV of isolated R3 (top), R4 (bottom), and R3 + R4 (middle) in the wind tunnel; R3 + R4 treatment replicates heterodyne interaction (U = 22.8 m s^{-1}). Heterodyne frequencies (purple arrows) produced in the wind tunnel include the integer harmonics of f_1, ($f_2 - 2\,f_1$, $f_2 + 2\,f_1$, $f_2 + 3\,f_1$) in addition to $f_2 \pm f_1$ recorded in the wild (B).

flutter and the induced sound, as has been hypothesized in the syrinx of chickadees (*14*). Allen's hummingbird (*Selasphorus sasin*, Fig. 4A), during its courtship dive, generates two simultaneous tones with R4 and R3 (Fig. 4B). The dive sound also includes heterodyne frequencies that disappear when either R4 or R3 is manipulated in wild birds (Fig. 4, B and C). We replicated the individual sounds of R4 and R3 separately in the wind tunnel, and then recreated heterodyne interaction frequencies in feather flutter and in the induced sound when R4 and R3 were placed in proximity (Fig. 4C). A third type of feather-feather interaction is collisions: In the Calliope hummingbird, multiple adjacent tail feathers are prone to torsional vibrations (Fig. 1H), causing neighboring feathers to strike each other, creating a sputtering sound during the species' display (*9*, *15*).

Our work shows that the tail of male bee hummingbirds functions as an acoustic organ, and we suggest that sexual selection through female choice for flutter-induced sounds has driven the evolution of diversity in male tail morphology (Fig. 2). The tail feathers are sexually dimorphic in shape, and males of each species have unique tail morphology. Small changes in feather mass, stiffness, size, and shape affect a feather's intrinsic resonant frequency, resulting in large changes in mode of flutter, acoustic frequency, harmonic structure, and which feather generates sound (Fig. 2). Nonlinear feather-feather aerodynamic interactions further expand the acoustic repertoire available to birds through flutter-induced communication sounds (Figs. 3 and 4), in such a way that they rival vocal diversity in many respects. For example, diving Allen's hummingbirds simultaneously produce two tones with the tail and a third sound with the wings (Fig. 4), an example of triphonation (production of "three-voiced" sound). These sounds may initially arise when sexual selection on acrobatic movements results in incidental flutter-induced sounds, which then become subject to novel mate preferences and incorporated into display repertoires (*16*).

The acoustic diversity in this hummingbird clade is a microcosm of the sounds feathers make across all birds. Tonal flight sounds are prevalent in the ordinary flight of birds with apparently unmodified feathers, including vultures, ravens, ducks, and loons, as well as the flights of arrows fletched with feathers (*17*), probably because all flight feathers are stiff, flat airfoils and thus prone to aeroelastic flutter above certain speeds, regardless of morphology. We hypothesize that acoustic communication signals produced by aeroelastic flutter have evolved many times in birds. Most birds that produce feather sounds in flight displays have multiple adjacent feathers with modified shape [such as flycatchers, guans, or woodcocks (*18*–*20*)], suggesting that the aerodynamically coupled interactions among neighboring feathers described here may be common. When the first birds took to the air, they had to contend with aeroelastic flutter. Although aeronautical engineers take extreme precautions to avoid flutter and its catastrophic consequences for aircraft (*2*), birds have instead repeatedly evolved novel acoustic communication signals from these incidental vibrations.

References and Notes

1. R. O. Prum, in *Peabody Museum Special Publication*, D. E. G. Briggs, Ed. (New Haven, CT, 2005), pp. 245–256.
2. R. L. Bisplinghoff, H. Ashley, R. L. Halfman, *Aeroelasticity* (Dover Publications, Mineola, NY, 1996).
3. A. Manela, M. S. Howe, *J. Sound Vibrat.* **321**, 994 (2009).
4. K. L. Schuchmann, in *Handbook of the Birds of the World. Vol. 5. Barn-Owls to Hummingbirds*, J. del Hoyo, A. Elliott, J. Sargatal, Eds. (Lynx Edicions, Barcelona, Spain, 1999), pp. 468–535.
5. J. A. McGuire, C. C. Witt, D. L. Altshuler, J. V. Remsen Jr., *Syst. Biol.* **56**, 837 (2007).
6. C. J. Clark, T. J. Feo, *Proc. Biol. Sci.* **275**, 955 (2008).
7. C. J. Clark, T. J. Feo, *Am. Nat.* **175**, 27 (2010).
8. T. J. Feo, C. J. Clark, *Auk* **127**, 787 (2010).
9. C. J. Clark, *Curr. Zool.* **57**, 187 (2011).
10. See supporting material on *Science* Online.
11. We did not detect both ranges IIIa and IIIb (Fig. 1B) in all of the feathers tested here because of a limited number of samples within range III. We hypothesize that all feathers would exhibit both IIIa and IIIb if tested with a dense U_{air} sample interval.
12. D. G. Crighton, *Prog. Aerosp. Sci.* **16**, 31 (1975).
13. J. W. Bradbury, S. L. Vehrencamp, *Principles of Animal Communication* (Sinauer, Sunderland, MA, 1998).
14. S. Nowicki, R. R. Capranica, *Science* **231**, 1297 (1986).
15. www.youtube.com/watch?v=265VdJRebzg.
16. R. O. Prum, *Anim. Behav.* **55**, 977 (1998).
17. L. E. Lauber, *Bowhunter's Guide to Accurate Shooting* (Creative Publishing International, Chanhassen, MN, 2005).
18. M. A. Traylor, J. W. Fitzpatrick, *Living Bird* **19**, 7 (1982).
19. W. G. Sheldon, *The Book of the American Woodcock* (Univ. of Massachusetts Press, Amherst, MA, 1967).
20. J. Delacour, D. Amadon, *Curassows and Related Birds* (American Museum of Natural History, New York, ed. 2, 2004).
21. C. J. Clark, *Proc. Biol. Sci.* **276**, 3047 (2009).

Acknowledgments: We thank T. Feo, A. McCallum, M. Girard, J. Windmill, J. Jackson, F. Montealegre-Z, the Prum lab, and three anonymous reviewers for input, and A. Varma for use of a photo. G. Weston-Murphy and M. Schmook kindly provided access to the wind tunnel at the Department of Mechanical Engineering, Yale University. Funded by NSF grant IOS-0920353 to R.O.P. and C.J.C. and NSF grant IOS-1021385 to D.O.E. Feathers were collected and imported under relevant permits. C.J.C. and R.O.P. initiated the project, C.J.C. collected and analyzed data, D.O.E. provided SLDV, R.O.P. provided support, and all authors contributed to the writing. Data are available from the authors upon request.

Supporting Online Material

www.sciencemag.org/cgi/content/full/333/6048/1430/DC1
Materials and Methods
SOM Text
Fig. S1
Table S1
Movies S1 and S2

7 March 2011; accepted 22 July 2011
10.1126/science.1205222